Segmentation of Medical Images with Adaptable Multifunctional Discretization Bayesian Neural Networks and Gaussian Operations

Original Scientific Paper

1. **Gomathi Ramalingam**
Department of Electronics and Communication Engineering,
University College of Engineering-Dindigul,
Tamilnadu, India
gomathiaudece@gmail.com

2. **Selvakumaran Selvaraj**
Department of Electrical and Electronics Engineering
PSNA College of Engineering and Technology,
Dindigul, Tamil Nadu, India

3. **Visumathi James**
Department of Computer Science and Engineering
Veltech Rangarajan Dr.Sagunthala R&D Institute of Science and Technology
Chennai, India

4. **Senthil Kumar Saravanaperumal**
Computer Science and Engineering Department,
Sethu Institute of Technology,
Virudhunagar, India

5. **Buvaneswari Mohanram**
Department of CSE,
Paavai Engineering College,
Namakkal. India

Abstract *– Bayesian statistics is incorporated into a neural network to create a Bayesian neural network (BNN) that adds posterior inference aims at preventing overfitting. BNNs are frequently used in medical image segmentation because they provide a stochastic viewpoint of segmentation approaches by producing a posterior probability with conventional limitations and allowing the depiction of uncertainty over following distributions. However, the actual efficacy of BNNs is constrained by the difficulty in selecting expressive discretization and accepting suitable following disseminations in a higher-order domain. Functional discretization BNN using Gaussian processes (GPs) that analyze medical image segmentation is proposed in this paper. Here, a discretization inference has been assumed in the functional domain by considering the former and dynamic consequent distributions to be GPs. An upsampling operator that utilizes a content-based feature extraction has been proposed. This is an adaptive method for extracting features after feature mapping is used in conjunction with the functional evidence lower bound and weights. This results in a loss-aware segmentation network that achieves an F1-score of 91.54%, accuracy of 90.24%, specificity of 88.54%, and precision of 80.24%.*

Keywords*: medical image processing, segmentation, Gaussian filtering, discretization*

1. INTRODUCTION

To classify each pixel in an image, image segmentation is an important and difficult topic. Segregation of covering noise using scan images to detect diseases, lung segmentation using computed tomography (CT) visuals to help distinguish between cancerous and benign lung lesions, edge detection of internal organs using eye scan images to detect disease premature, and image segmentation for surgical preparation are just a few of its many uses [1]. It is highly difficult to accomplish precise and consistent separation of defects in medical imaging that are substantial variations in the outline or dimensions of the pathophysiology across people, although there may be a poor distinction between the classification target and adjacent tissues. It has been a few years since deep neural networks (DNNs) surpassed human specialists in several medical image segmentation tasks.

Decisions on how to segment an image are decided solely by the model, and this might lead to inaccurate predictions. Reliability is critical in areas like medical

diagnostics and self-driving car technology, where mistakes can have devastating effects if they are made in life-threatening conditions. The lack of interpretability of DNN predictions has led many to dismiss these systems as black boxes. Finally, the deep architectures used by DNNs may lead to overfitting as a result [2]. As a result, huge datasets and regularisation procedures are needed to thwart this trend. As an alternative, Bayesian neural networks (BNNs) might do away with the shortcomings of deep neural networks (DNNs) altogether.

For a BNN to be accurate, it must consider the uncertainty in its predictions, hence it treats weights and biases as random variables. Using a scalable methodology, these models help to minimize overfitting and to provide a sense of uncertainty. A disciplined approach to predicting and interpreting model outputs using BNNs is made possible by this method. Medical image segmentation relies heavily on uncertainty estimates since it may shed light on the level of confidence in a segmentation's conclusions and so assist doctors to make better diagnoses [3]. As a result of the requirement to use such approaches in real-world systems, researchers have become increasingly interested in deep learning and learning with Bayesian networks. BNNs are often trained using variational inference (VI), which transforms normal Bayesian learning into an optimization issue. Steps in the Medical image processing framework are shown in Fig. 1.

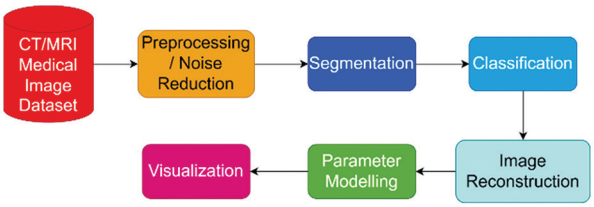

Fig. 1. Steps in Medical image processing framework

Approximating the posterior is easy using VI since it allows you to choose a vaguely resembling probability distribution and then optimizes it. Kullback–Leibler (KL) divergence may be used to quantify how close an estimate and the genuine subsequent models are, and reducing this discrepancy is comparable to normalizing the adverse indication lower limit. Based on VI, it's easy to build BNNs and they're resistant to overfitting. Graves presented a method to evaluate a factorized subsequent or a partial calculator using data subsampling techniques. This made it possible for the method to handle vast volumes of data [4].

An effective stochastic gradient VI technique, known as Bayes by Backprop (BBB), was devised by Blundell et al. based on this to measure weight uncertainty. The use of Gaussian approximation distributions indeed results in a larger number of model parameters, which makes this variational technique less suitable for usage with big complicated models than prior variational approaches [5]. The model quality and uncertainty estimate of probabilistic backpropagation and approximation inference approaches that rely upon deviation reduction take greatly enhanced over these VI techniques. However, the enormous processing costs, scale, and nonlinearity make these VI techniques computationally infeasible.

GPs provide exact estimates of uncertainty for trustworthy forecasting, also the association among GPs were already been widely investigated. Neal claims that when the BNN width grows, GP is the limiting distribution. The system having dropping levels is analogous to approximation for dynamic modeling with Monte Carlo (MC) simulations in the forecast at runtime. Using the Monte Carlo dropping (MC-Dropout) technique to deep GPs may be seen as a Bayesian calculation. They share a commonality of deep structures, which explains their close association. According to Ma et al., BNNs provide a contained randomized development, and for applying variational methods for training and reasoning throughout a functional domain, BNN models are established.

An investigation of the VI between GPs led Sun et al. to create functional variational BNNs (FBNNS) that are used to specify an aim and to estimate the role at limited inputs. Carvalho et al. introduced a GP variational family technique based on the fELBO goal, which allows functional VI to be used for high-dimensional feature extraction problems. For every network design, this approach delivers well-calibrated uncertainty estimates and only one forward pass is required for predictive inference [6].

In the case of limited hyperparameters and a big dataset, the query optimizer prefers to optimize the aggregate log-likelihood component rather than the negative log-likelihood. As a result, determining the optimal hyperparameters will be difficult [7]. It is also computationally difficult when utilizing powerful BNNs to compute the model posterior, culminating in systems that are costly to run. Many people have worked to develop BNNs that can both scale and estimate. When it comes to segmenting medical images, the model's performance is hampered by intricate border interactions, greater visual variability, and low extracellular matrix contrast [8].

Consequently, the identification of the most significant attributes is critical to the model's effectiveness. Here, we introduce a reliable FBNN that does medical image segmentation to overcome these concerns. Variational inference is performed on the posterior and variational prior probabilities, which we refer to as GPs. The value obtained from the KL deviation unit is analogous to the adverse log probability when using a threshold with KL deviation in the variation. Rather than immediately increasing in proportion to the number of variational parameters, the KL divergence grows as the quality of the discretization parameters improves. As a bonus, we present a medical image segmentation that is cognizant of content [9].

Feature upsampling uses content-aware reassembly of features to retrieve semantic data from input feature maps, which improves model performance while decreasing computational costs. With one forward pass, the suggested BNN may perform predictive inference in high-dimensional problems. This technique outperforms several current Bayesian models for segmentation evaluation criteria and confidence approximations on open medical image data sources.

The research work proposed in this article possesses the following key contributions: To assist the model in discovering the most optimum variational parameters, we present a weighted version of the loss function parameter model in function space. An adaptive framework is presented for the segmentation of medical images. When building this model, we took advantage of a computationally efficient up-sampling component. Experiments were conducted with the openly available dataset that shows that the proposed model outmatches several current approaches in terms of segmentation performance measures and uncertainty estimations.

2. LITERATURE SURVEY

In the field of medical image segmentation, UNet has achieved greater success. FCNs are used to create a novel architecture in this network. With this UNet design, numerous better segmentation processes, like as residual as well as dense mechanisms, have been presented. An algorithm created by Isensee et al., called nnU-Net, can autonomously arrange itself for any biomedical job, encompassing pre-processing, network design and training, and post-processing. nnU-Net is a free, open-source technology that outperforms most existing techniques [10]. For the COVID-19 lesion region, a content-aware residual UNet was proposed by Xu et al.

Segmentation results are more accurate and computational costs are reduced with this approach. There is no probability calculation for the segmentation findings of these vanilla DNNs, thus they make judgments only based on point prediction. In image segmentation, BNNs generate predictions for each pixel as well as estimations of pixel-wise uncertainty. When it comes to making decisions, it's critical to consider the principles of uncertainty. Deep ensemble methods and Bayesian approximation are the two most used approaches to quantifying segmentation ambiguity in biomedical imaging using BNNs [11]. As a strong approach for assessing uncertainty, the deep ensemble assesses the model's uncertainty by training numerous models and collecting their output predictions' variances, which are then averaged together.

On two publicly accessible echocardiography datasets, Dahal et al. examined various ensemble-based indecision approaches. Four metrics were used to measure uncertainty and show how uncertainty estimates are done automatically and enhance the outcomes. They were shown to be effective [12]. Since BBB and other typical Bayesian approaches cannot accurately approximate the average Bayesian model, Wilson and others have shown that deep ensemble models can. Dropout is a regularisation term in the MC-Dropout technique of Bayesian approximation, which is commonly used in medical imaging applications to quantify the prediction uncertainty [13]. This approach is widely used since it is simple to implement.

As a result, weight perturbation-based methods suffer from large variations in gradient estimation since they use the weight space's intractable prior and parameterized a GP as the discretization posterior [14]. CNN was used for the GP prior kernel and the GP posterior kernel. There are issues with their approach, however, such as the inability of fELBO loss to get the optimum solution in function space in all cases and the enormous computing cost. CARAFE is used as an optimized feature average pooling operator in the CAUNet, unlike the other Bayesian approaches discussed [15]. Competingly efficient, the suggested segmentation approach enhances model performance indicators and uncertainty estimations.

It is vital to segment important items in medical images and extracts information from segmented sections to aid physicians in making correct diagnoses. Feature extraction, clustering approaches, bayesian hierarchical frameworks, dynamic patterns, computer vision, etc. are common in early medical image segmentation approaches. An updated edge identification approach based on mathematical morphology was proposed in [16] for CT scans of the lungs. Disc inspection using Hausdorff-based template matching was performed by [17], while ventricular fragmentation in brain CT images was accomplished using a similar method by [18].

To segment cardiac MRI images in 2D and prostate MRI images in 3D, [19] suggested a shape-based technique using horizontal sets. Liver tumors in abdominal CT images were segmented using the activation profile model by [19], while [20] designed a methodology for medical anatomy data segmentation using level sets and SVM classifiers (Support Vector Machines). Brain MRI images were segmented using Markov random fields (MRF) by Held et al. Image segmentation is still one of the most demanding subjects in computer vision owing to the difficulty of feature representation, even though several algorithms have been described and are successful in specific conditions.

Because of issues like a blur, noise, low contrast, etc., medical images make it more difficult to extract discriminating characteristics than standard RGB images [23]. Convolutional neural networks (CNN) accomplish hierarchical visual features of images, making medical image segmentation the hottest research area in image processing and computer vision thanks to the rapid growth of deep learning techniques. Thanks to the robustness of CNNs for feature learning, medical image segmentation is not negatively impacted by common

image artifacts such as clutter, distortion, sharpness, etc. Semantic segmentation and instance segmentation are the two main types of image segmentation tasks now in existence [24].

Image segmentation is used as a probabilistic classifier that labels each pixel in an image with a certain category. Instance segmentation, in contrast to semantic segmentation, requires not just pixel-level categorization but also the ability to differentiate instances based on specified categories. Since every organ and tissue is unique, there have been surprisingly few papers on detection and segmentation in healthcare image segmentation [25]. We take a look back at the progress made in applying deep learning to the task of segmenting medical images. Machine learning is generally broken down into subfields called supervised learning, semi-supervised learning, and unsupervised learning based on the availability of labels for training data. It is challenging to get a significant amount of labeled data for medical imaging, despite supervised learning's benefit of training models based on correctly tagged data.

Unsupervised learning, on the other hand, can be done without labeled data, although it is more challenging. Weakly supervised learning bridges the gap between supervised and unsupervised learning by simply requiring a subset of data to be labelled [26]. Medical image segmentation had previously been the subject of several model-driven techniques reported by researchers before deep learning's mainstream adoption. Image clustering, region analysis, and random forest are only a few examples of model-driven approaches in medical image analysis that were summarised in detail by [27]. Using a variety of mathematical models, the authors of [21] summarised the many techniques used to do segmentation on medical images.

For medical image segmentation, only a small number of research using model-driven approaches have been reported recently, whereas an increasing number of studies are using data-driven techniques. The growth and improvement of deep learning models for medical image segmentation are the primary topics of this research. Shen et al. gave a comprehensive study of deep learning's use in medical image processing [28]. Here, we take a look back at how far we've come with computer-aided illness diagnosis and prognosis, tissue segmentation, machine learning, and deep learning in the field of medicine. An overview of deep learning approaches was recently given by [29], which discusses the application of deep learning to various tasks such as image classification, object identification, segmentation, registration, and more [22].

The recent growth of semantic and medical image segmentation was discussed by [30], who divided deep learning-based image segmentation alternatives into six categories: deep modern architecture, data biosynthetic pathway, loss function-based, sequential models, weakly carefully monitored, and multi-task approaches. In [31], the authors evaluated artificial neural networks (ANNs), convolutional neural networks (CNNs), and recurrent neural networks (RNNs) as well as classical machine learning algorithms like Markov random fields, k-means clustering, and random forest to create a more comprehensive survey on medical image segmentation (RNNs). Solutions for medical image segmentation with incomplete data sets were evaluated by the authors of [32], with the authors highlighting the constraints of both sparse and weak annotations as important obstacles. All of these surveys are crucial to improving medical image segmentation methods.

The methodologies such as network architecture, training methods, and difficulties were all covered in [33]. This article breaks down the most well-known and widely-used network architectures for image segmentation. The J Digit imaging method for training deep neural network models is covered in the section devoted to training methods. The problems of employing deep learning algorithms for medical image segmentation are described in detail in the next section. In a recent study, the researchers [34] examined the progress made in applying deep learning to chemotherapy and the possibilities for its future use. In their recent article, the authors of [35] summarised the state-of-the-art methods for quantitative brain MRI image segmentation using deep learning. Incomplete supervision, inexact supervision, and incorrect supervision were the primary areas of concern [36]. Optimizing approaches for medical image semantic segmentation are evaluated and summarised by Eelbode et al. [37], with a particular emphasis on Dice scores as well as Jaccard values.

2.1 RESEARCH GAP

Unfortunately, there is a critical flaw in the formulation that prevents the loss from always leading to appropriate variational parameters when adopting existing approaches. Two factors, the inverse log-likelihood as well as the deviation among the Bayesian approximation that the prior distribution, contribute to the optimization of the specified loss, and their relative importance is determined by the size of the collection and the model's parameters [16]. When training a model with few parameters using a large dataset, the continuous random variable likelihood will initially be very high, whereas another term will be extremely low. It is expected that the optimizer will give priority to the log probability term. Consequently, identifying the best values for the model parameters will be challenging [17].

In addition, the inference of the model posterior is computationally intractable, and powerful BNNs often have a high number of parameters, leading to computationally costly models. Consequently, a lot of effort has gone into creating approximation BNNs that can scale well [18]. Last but not least, the medical image segmentation job has its unique challenges due to the complicated border interactions, increased appearance variance, and poor surrounding tissue contrast.

That's why it's crucial to accurately extract the most relevant features for the model to work.

3. SYSTEM MODEL

Here, we quickly examine a generic explanation and then present the probabilistic VI design, and operational VI. Let us now turn our attention to what we refer to as content-aware upsampling.

In a chosen dataset that comprising of pairs of data denoted by $D=\langle a_x, b_{ox} \rangle$, where x is ranging from 1 to P. The objective variable a_x is a scalar, and we have a total of P observation data pairings where D is the feature vector and $b_x \in Q$ are the feature matrix, and these are represented by a_x and b_x, respectively. Neural networks are used in parametric regression, where a collection of parameters (a) is used to define an appropriate function for the inputs and outputs (b) of the neural network. A prior probability over through the domain of system parameters was inserted in BNNs, where weights and biases are considered random variables, and the weight matrixes for each layer are treated as random variables. This prior distribution is a prediction of which parameters may have created the results before any data was observed. The probability over parameter space was calculated by applying Bayes' theorem to a set of statistically independent observations, i.e., D. $P(A \mid B)$ defines the conditional probability, and $P(A)$ and $P(B)$ are the associated probability of A and B.

$$P(A|B) = \frac{P(B|A)P(A)}{P(B)}, \quad (1)$$

where $P(B)$ has been estimated as,

$$P(B) = \int P(B|A)\ P(A)\ dA, \quad (2)$$

$$\text{and} P(B|A) = \prod_{x=1}^{P} P(a_x|b_p, A) \quad (3)$$

which represents the normalization component and the log-likelihood value respectively. The parameters of the network that are most likely to be affected by the observed data are represented by the probability density. Assuming a SoftMax probability for the classification problem, we may conclude that,

$$P(a_x = d|a_x, B) = softmax(g(a_x{:}B)) \quad (4)$$

$$\text{as·well·as·} P(b_x|a_x, B) = \mathcal{G}(b_x; g(a_x{:}B), \mu^2 J) \quad (5)$$

for the assumed data pairs.

Image segmentation and tracking have received a lot of emphasis from deep learning applications, but the recognition system hasn't received the same level of attention thus far. Though several promising works have been published, this does not mean there aren't a lot of possibilities. In point-based registration, finding good features extracted that allow for the proper identification of associated points is a common difficulty. The difficulty of finding a specific constituent in a medical image is addressed by image detection and recognition. The images are often volumetric. Consequently, fast parsing is essential.

The most common method is marginal space learning, which is both efficient and resilient in detecting organs. To make it even more efficient, its deep learning counterpart uses a computer vision boost cascading instead of a probabilistic tree. Still, the complete volume must be processed to accurately identify anatomical features. Using deep reinforcement learning, the search process may be replaced by an artificial entity that explores anatomy to identify anatomical structures. In only a few seconds, the approach can identify hundreds of landmarks throughout a complete dataset.

Because it lacks a closed-form equation, the real posterior distribution could be computed analytically in practice; an approximation must be employed instead. The posterior is frequently approximated using VI. Free variational parameters are used to construct an approximate variational distribution. In addition, the parameters of the approximation distribution and the real posterior are modified to minimize the dispersion.

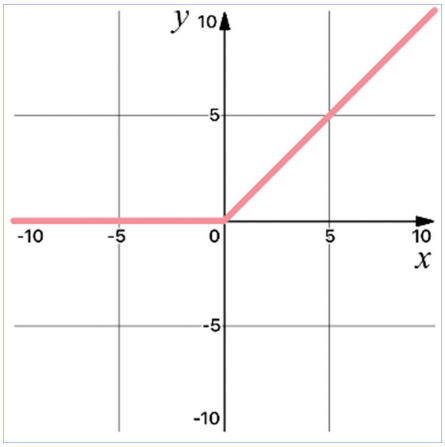

Fig. 2. Activation Function

$$\hat{\rho} = argmin_{\rho}(\mathcal{G}(b_x; g(a_x{:}B)) \quad (6)$$

Decreasing the negative parameters is the same as minimizing the KL divergence, as shown by the equation. Due to BNNs being highly nonlinear, this equation cannot be used to compute h analytically. It's possible to lower the volatility of the baseline predictor for the discretization of BNNs by using the re-parametrization approach, which has just been developed in VI. This technique, known as re-parametrization, was used to choose samples from the discretization distribution in which a point-wise combination and the standard deviation are nonnegative and may be represented. The loss function may be estimated by combining the re-parametrization method with an MC approximation.

The up-sampling approach has three advantages. It has a wide field of view, is inexpensive and fast to calculate, and is content-aware. A parameterization activator with content-aware kernels enhances the effectiveness in object identification, classification techniques, and

texture features compared to traditional benchmarks. We use the following steps to accomplish upsampling. When compressing the input feature channel, we first used a convolution layer. The reassembly kernels were then encoded depending on the content of input features using a second higher-order convolution layer. SoftMax function was performed on each reassembly kernel geographically before upsampling to ensure that all kernel values were equal. Upsampling does not rescale or modify the average scores of the convolution layer because of normalization. It is possible, to sum up, the kernel forecasting component in this way:

$$Y_g = V(C_{3\times3}(C_{1\times1}(a_x))) \cdot \tag{7}$$

where the convolutional with the kernel is denoted by the symbol C. One pixel in a kernel has the location in the feature map, which is the result of the content encoder operation. V is the algorithm that works the view of the underlying Kernel, and a_x is the feature map after the information encoder. As a final step, we reconstruct the characteristics into anticipated kernels, which we may represent as kernels.

3.2 PROPOSED MODEL

Autoencoder and linear interpolation blocks comprise the Bayesian antecedent system. Extension of the model that takes advantage of the encoding-decoding structure. We use the model as a feature upsampling operator instead of a separate feature extraction tool. Using convolutions instead of pooling processes result in connections with a smaller memory footprint when training because no switches are required to map the output of the pools back to their inputs. Additionally, networks with smaller memory footprints can be effectively understood and analyzed by using only deconvolutions instead of unspooling operations. For the following network layers, we can use a larger receptive field with less signal complexity by downsampling input data.

During each step of the network's left side, two times as many features are calculated as the preceding layer. Feature extraction and spatial expansion of lower-resolution feature maps are performed in the right section of the network so that the essential information may be assembled to produce a two-channel volumetric segmentation. We use soft-max voxelwise mostly on feature space maps obtained by the final fully connected layer, each with a 1×1 kernel size, to produce randomized segmentation of their original image regions. There are one to three convolutional layers, each with half the average of 5 × 5 × 5 kernels, that follow each phase of the CNN's efficient distribution channels. This increases the input data size. It's just like on the left side of the network, where we use residual functions to learn in the convolutional phases.

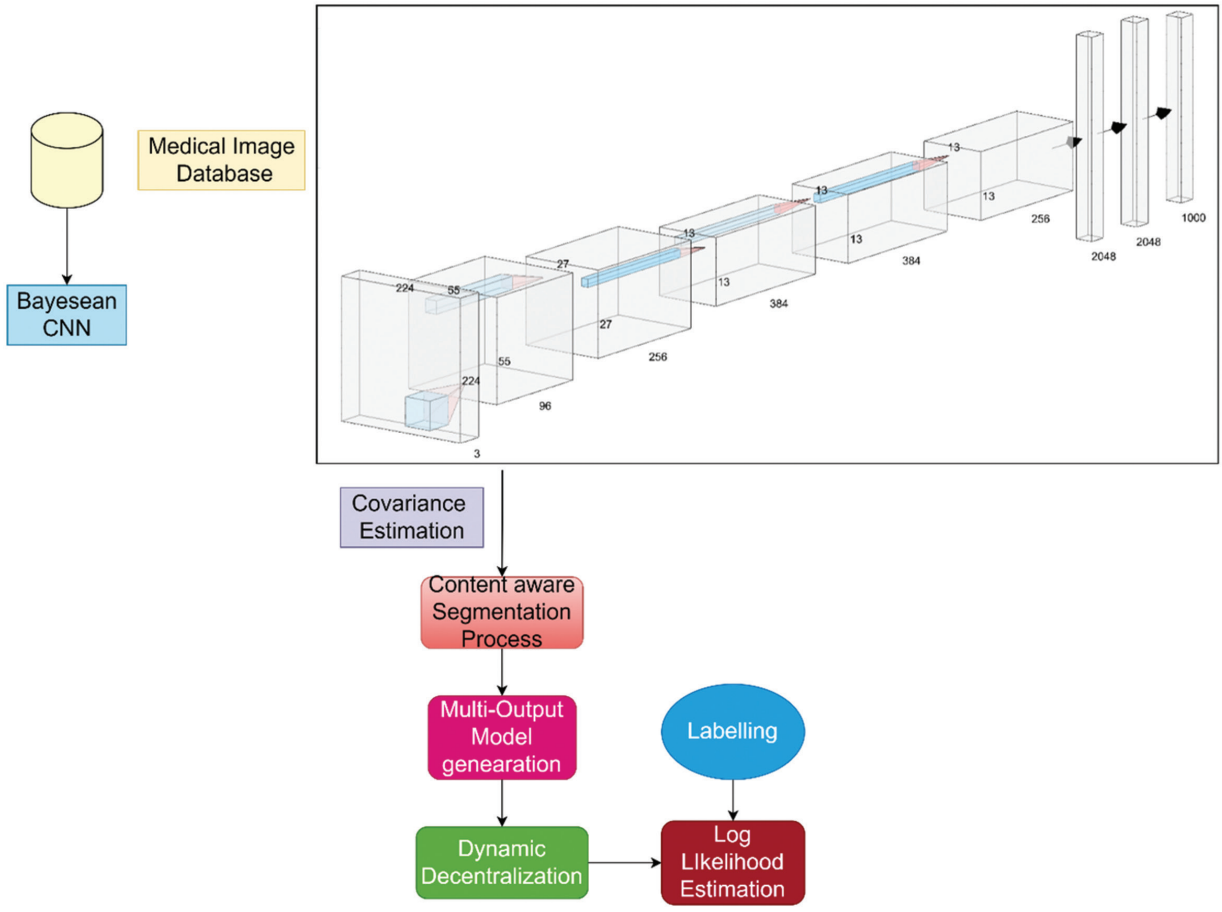

Fig. 3. Proposed image segmentation model architecture

Of the identical accuracy as that of the initial input data, the system recommendations in two dimensions are processed by a softmax layer. To determine the possibility of each voxel being in the foreground or background, each layer provides the probability. In medical datasets like the types we're dealing with, the architecture of interest is often only a small percentage of the scan. An untrained network will be significantly biased towards the background because of this, and learning will become stuck at the global optimum of the gradient descent. Consequently, the foreground is sometimes absent or just partially discernible. Sample reweighting was used in several earlier ways to reduce loss functions where foreground areas were given greater weight than ambient ones during learning.

Our goal is to maximize the coefficient that takes a number between Zero and one in this research, which we define as an objective function. It is unnecessary to weigh a variety of various classes when using this formulation, and the results obtained are superior to those obtained through another network trained to optimize a logistic regression loss with sample reweighting, as we have experimentally observed. This is because we don't have to weigh samples of different classes. A ReLU activation function and the CNN precondition model are also employed. The correlation coefficient H can be calculated accurately by a Bayesian CNN with arbitrarily numerous convolutional filters, which are identical.

$$\mathcal{M} = \rho LM[r(g^{y})|| \, q(g^{y})] - \sum_{j=1}^{M} \wp_{r0}(g(y_j)) \left[\log q \, (z_j[g(y_j)]\right] \tag{8}$$

Additionally, it is possible to get the inverse correlation matrix and eigenvalue of K. Thus, the kernel for segmentation tasks was included in the design. This KL divergence component may be computed using mappings that have been parametrized. A kernel matrix represents a square matrix for massive Bayesian CNNs because of the zero pixel-pixel correlations in Bayesian CNNs without pooling layers. Images with dimensions H and W that have C layers can be used as inputs to the algorithm.

$$\sum_{mn} \frac{1}{M} \sum_{l=1}^{M} f_l(a_m) \oplus f_l(a_n) + G(a_m, a_n)\rho(a_m, a_n) \tag{9}$$

We utilized a loss function that is inverse to the BNN's true loss value to train it. KL term size and log-likelihood term expectations are both dependent on the dataset and model parameters. KL divergence can be substantially larger than low log-likelihood when the dataset is small but the model has many parameters. Optimizers will always favor high-value terms over low-value ones in these two scenarios. This means that it will be hard to get the best dynamic features for CNN. Consequently, a b-weighted loss function has been included to overcome this issue.

The extra expanding route, multi-dimensional identity process, and dissimilar multi-scale convolutional blocks are the three key additional advanced components in the suggested model compared to the standard U-Net. To enhance the model's learning power through dual supervision, a new, expanding path is developed to introduce a new learning loss, namely, auxiliary loss. Since the suggested approach incorporates both the image features from the convolution layer and the intermediary classification values from the extra expanding path, it can produce more precise segmentation results. In addition, the suggested model suggests a strategy to deal with the issue of irrelevant information by employing two successive self-attention components, dense space orientation focus, and connection recognition, to capture the significance of characteristics in both the positional and multichannel aspects.

Applying a dilated convolution block in the model, the input feature map is transformed into a dense feature matrix of reduced size, which is then utilized to estimate the spatial dependencies, allowing for efficient estimation of the weights of features in the spatial structure. Furthermore, the proposed model's blocks are put to use to address the semantic gap through the usage of multiscale convolution kernels that are coupled in a variety of ways (series and parallel) to accommodate for the differences in convolutional size. Thus, the created multi-scale feature maps may be used more effectively, and the combined feature maps can better minimize semantic discrepancies since they maintain more extensive semantic information with varied scales. The model was designed to segment 2D medical images, but it can be readily expanded to a 3D model to analyze 3D medical images in a manner analogous to how U-Net can be extended to a 3D model.

The initial upgrade to the model is the inclusion of an extended path to U-Net so that dual supervision may provide more precise results when segmenting medical images. Specifically, the suggested model contains just a single contracting route, like U-Net, but unlike U-Net, after the most speculative characteristic mappings have been collected at the innermost part of the convolution layer, they are transmitted to two expanding pathways with identical topologies. Both the previous expansive path, which was already present in U-Net and the new expansive path, which was just introduced, have names.

Similar to the skip connection operation in U-Net, we combine the feature maps produced by the corresponding layer of the convolution layer with the feature maps produced by the transfer function fully - connected up-sampling operations in the final layer to create the feature maps used in the additional expansive path. The new expansive path's combined feature maps are then given to the layer that follows it, as well as the layer that the initial expansive path maps to. As a result, the unsampled feature maps from the new expansive path are added to the feature maps again from the convolution layer and the original expansive path

in each layer. Last but not least, the supplementary expansive path is used to train the deep model using a pair of segmentation losses, one from the primary extensive channel and one from the supplementary extensive channel.

There are two types of uncertainty in BNN predictions: perceptual and aleatoric. Model uncertainty, another name for ambiguity, is a way of quantifying the unknown. This makes evaluating Bayesian uncertainty estimation difficult because there is no integral gain for the estimations. To assess the models' ability to estimate uncertainty, we combined the ground truth label with predictions from the target model and predictive entropy. The consistency map and the confidence map are necessary to compute these metrics. Accordingly, the correctness and uncertainty maps may be calculated by matching the regression coefficients labels and model predictions, respectively. The four types of evaluations are False Positive (TP), True Negative (TN), False Positive and False Negative (FP), and True Negative (TN) wrong and certain (False Negative, FN).

4. RESULTS AND DISCUSSION

The lung segmentation dataset was the subject of several investigations. The Kaggle Data Science Bowl presented the lung segmentation dataset in 2017 [38]. There are two- and three-dimensional CT images with lung segmentation labels labeled. There is a total of 512×512 pixels in each image, so it's rather detailed. The lung region was isolated from the surrounding areas and the images were divided at random into three sets: training, validation, and testing. We utilized 450 training images, 120 validation images, and 400 testing images in this work. There was an 8-node Bayesian CNN GP preceding network with weight and bias basis functions with variances of 0.2 and 0.08. Content-aware upsampling used the same hyperparameters.

To verify that the transverse members of the covariance matrix are not zero, we set L to 0.30 and included a threshold value of 1.03 to the transverse. We had an initial learning rate of 0.01 a weight decay rate of 0.04, and an annealing factor of 0.998, the optimization technique used stochastic gradient descent (SGD). We trained in batches of four, and for the DRIVE dataset, we trained in batches of twenty patches. Systems were accomplished for 200 epochs for segmentation experiments. Here, the proposed models were trained for 125 epochs. A Linux computer with a Geforce P5000 GPU was used for the tests, which were carried out using PyTorch for all of the models. There are several different baselines against which we might measure the suggested approach's efficacy and superiority. BNN's GP prior in feature space is the inspiration for our concept.

As a result, this method was the most natural starting point. All of these deep learning inference methods use an approximation of Bayesian inference and express uncertainty naturally. It is possible to assess uncertainty in a model using a deep ensemble. Class-likelihood estimates are produced by the UNet design with a softmax output layer, and this architecture may express the network's uncertainty. Non-Bayesian uncertainty quantification approaches such as Softmax and Deep Ensemble are frequently employed. Moreover, to properly test the influence of various parameters of b upon segmentation efficiency, we applied the described segmentation method.

Table 1. Performance analysis with existing models

	F1-Score	Accuracy(%)	Specificity	Precision
Softmax	**0.8798**	**85.78**	**0.8154**	**0.7854**
FBNN	**0.8547**	**85.78**	**0.8124**	**0.7754**
Proposed	0.9154	90.24	0.8854	0.8024

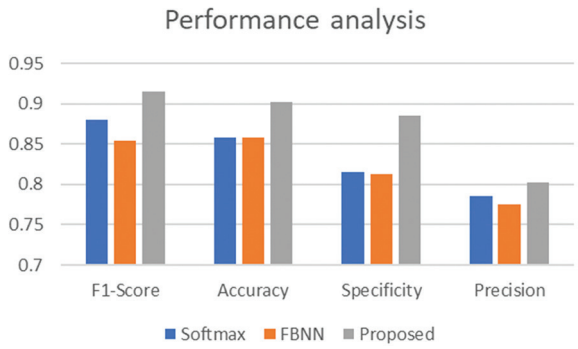

Fig. 4. Performance analysis

So that all models could be compared fairly, we chose the same UNet design, which consists of five encoder and decoder blocks. The dropout frequency was adjusted to 0.2 for MC-Dropout in the ensemble of four identical UNets. Mostly from the dataset of lung segmentation, the various approaches are evaluated. For this test set, the results were obtained by utilizing the suggested and baseline procedures. In this dataset, our technique surpassed all of the baseline methods, notably precision, our method's outcome is somewhat better than that of both b1 and b2. MC-Dropout was the poorest of the test outcomes. The superiority of our strategy in comparison to this dataset shows that the suggested method is useful in increasing the model's performance and generalization capacity.

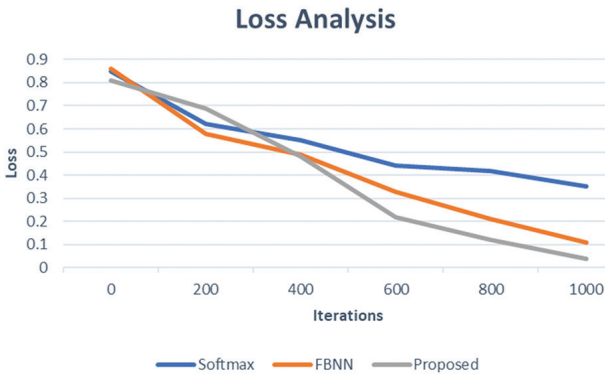

Fig. 5. Loss Analysis

Estimated ROC curves are used to demonstrate the overall efficiency of the suggested and baseline approaches on the four datasets. The true positive rate (TPR) is shown alongside the false positive rate (FPR). The more accurate a model is, the closer the ROC curve gets to the top-left boundary of the coordinates of ROC. In terms of techniques, the b2 slope is perhaps the most left-leaning among them. Figures also demonstrate that our technique has the biggest area under the ROC curve compared to the other methods (AUC). That our approach works better than others is further supported by these findings. Using a variety of Bayesian frameworks and datasets, a qualitative analysis may make use of the outcomes of segmentation and uncertainty in the models.

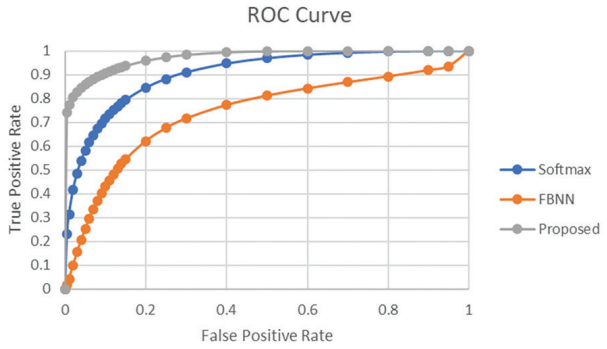

Fig. 6. ROC curve Analysis

This target's contours aren't well-segmented when using Prob. UNet, MCDropout, and FBNN predictions against the respective ground truth labels. Our approach has a segmentation boundary that is closer to the real world than the baseline methods do. When used on the lung segmentation dataset, MC-Dropout and SWAG both under-segment and under-represent the overall shape. In the lung segmentation test, our solution outperformed the standard methods by a wide margin. Aside from this, the suggested approach was able to properly detect and segment the existence of vessels in blood and the images of the retina. Small blood arteries, on the other hand, did not segment effectively using the baseline approaches.

Table 2. ROC Formulation

FPF	TPF	Lower	Upper
0.005	**0.2301**	**0.0169**	**0.7407**
0.01	**0.3135**	**0.043**	**0.7718**
0.02	**0.4168**	**0.0996**	**0.8061**
0.03	**0.486**	**0.1545**	**0.8282**
0.04	0.5384	0.2056	0.8449
0.05	0.5807	0.2523	0.8587
0.06	0.6159	0.2949	0.8705
0.07	0.6461	0.3337	0.8808
0.08	0.6723	0.369	0.8901
0.09	0.6955	0.4012	0.8985

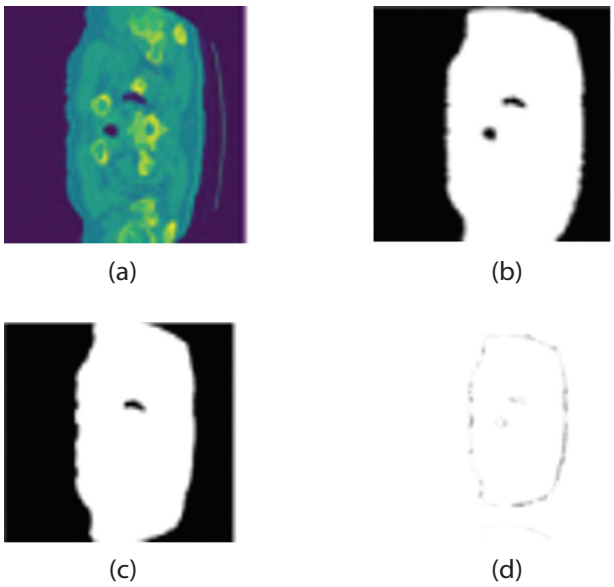

Fig. 7. Segmentation Outcomes: (a) Original (b) Edge detection (c) Region identification (d) Segmented Features

The incorrect and uncertain pixels are highlighted in the correctness and confidence maps, respectively. The confidence maps for various approaches in the image show that models usually have considerably larger ambiguity for the boundary of the classes, which indicates that the model underperforms over these classes. A high level of confidence is also found in pixels that are distant from the edge of the screen. It can be observed from the figure's correctness maps that wrong areas tend to be located along the boundaries of classes. These findings show that models typically produce large uncertainty estimations when the forecast is incorrect. When compared to the baseline approaches, all segmented regions, even accurate regions, are subject to considerable uncertainty. Overall, our technique outmatches the baseline methods in terms of segmentation and estimations of uncertainty.

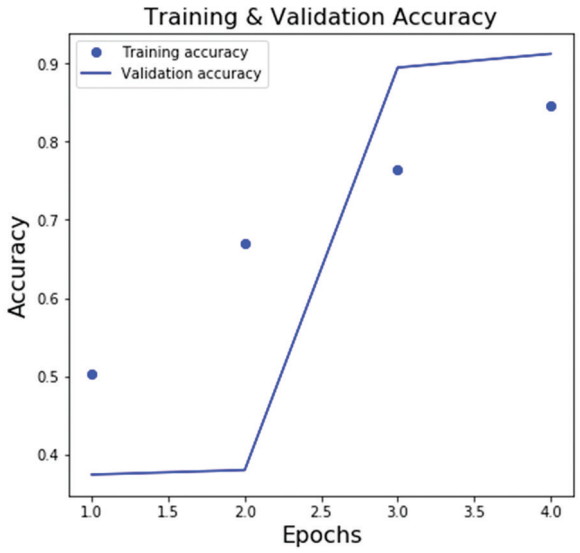

(a)

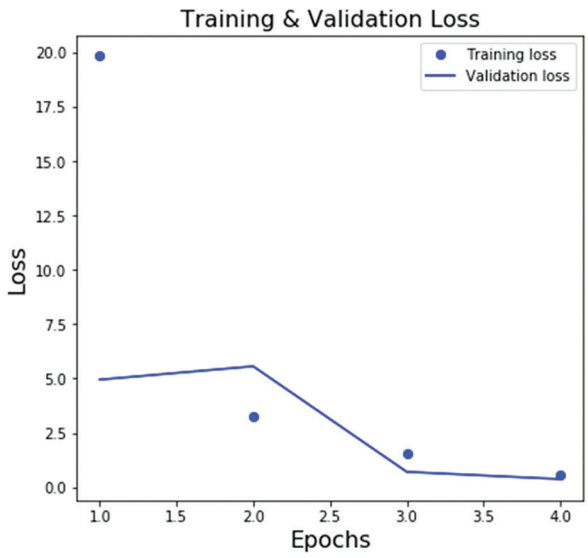

(b)

Figure 8. (a) Training and validation Accuracy (b) Training and validation Loss

5. CONCLUSION

A reliable method for segmenting medical images has been discussed in this research paper. This can be defined as the distribution function and the variational posterior of the variational goal. It was possible to train BNNs with GPs by using a model variation that included a b-weight mostly on KL deviation unit for the functional VI goal, which we presented. A CNN that takes advantage of the downsampling operator to enhance model performance while lowering computing costs was also presented. The proposed approach outperforms current methods in terms of reliability, ambiguity prediction, and accuracy, according to the findings of the assessment studies. The performance is restricted by the function before and the parameterization of the likelihood function. The Bayesian CNN prior network must be properly designed, and the finite difference posterior must be precisely parameterized.

As shown by the experimental findings, the suggested technique achieves better performance, uncertainty estimates, and inference time than the state-of-the-art methods. This results in a loss-aware segmentation network that achieves an F1-score of 91.54%, accuracy of 90.24%, specificity of 88.54%, and precision of 80.24%. We need to carefully build the Bayesian CNN GP prior network and parametrize the variational posterior to maximize the suggested method's performance, which is constrained by the stated function before and the parameterization of the posterior distribution. We hope to improve upon our current technique of parameterizing the covariance of the posterior distribution and investigate the potential of applying it to the segmentation of 3D medical images in the future. The automated configuration of a BNN like nnU-Net, including pre-processing, network design, and training for medical image segmentation, presents a significant challenge.

6. REFERENCES

[1] X. Chen, Y. Zhao, C. Liu, "Medical image segmentation using scalable functional variational Bayesian neural networks with Gaussian processes", Neurocomputing, Vol. 500, 2022, pp. 58-72.

[2] S. D. Halle, D. N. Dunn, A. H. Gabor, M. O. Bloomfield, M. Shephard, "Bayesian dropout approximation in deep learning neural networks: analysis of self-aligned quadruple patterning", Journal of Micro/Nanopatterning, Materials, and Metrology, Vol. 21, No. 04, 2022.

[3] J. Steinbrener, K. Posch, J. Pilz, "Measuring the Uncertainty of Predictions in Deep Neural Networks with Variational Inference", Sensors, Vol. 20, No. 21, 2020, p. 6011.

[4] T. Hussain, "ViPS: A novel visual processing system architecture for medical imaging", Biomedical Signal Processing and Control, Vol. 38, 2017, pp. 293-301.

[5] C. Villacampa-Calvo, D. Hernández-Lobato, "Alpha divergence minimization in multi-class Gaussian process classification", Neurocomputing, Vol. 378, 2020, pp. 210-227.

[6] Y. Li, Q. Zhang, S. W. Yoon, "Gaussian process regression-based learning rate optimization in convolutional neural networks for medical images classification", Expert Systems with Applications, Vol. 184, 2021, p. 115357.

[7] A. Maier, C. Syben, T. Lasser, C. Riess, "A gentle introduction to deep learning in medical image processing", Zeitschrift für Medizinische Physik, Vol. 29, No. 2, 2019, pp. 86-101.

[8] S. Bansal, "Determining Disease Using Machine Learning Algorithm in Medical Image Processing: A Gentle Review", Biomedical Statistics and Informatics, Vol. 6, No. 4, 2021, p. 84.

[9] R. Wang, T. Lei, R. Cui, B. Zhang, H. Meng, A. K. Nandi, "Medical image segmentation using deep learning: A survey", IET Image Processing, Vol. 16, No. 5, 2022, pp. 1243-1267.

[10] B. Wiestler, B. Menze, "Deep learning for medical image analysis: a brief introduction", Neuro-Oncology Advances, Vol. 2, Supplement_4, 2020, pp. iv35-iv41.

[11] A. Mobiny, P. Yuan, S. K. Moulik, N. Garg, C. C. Wu, H. Van Nguyen, "DropConnect is effective in modeling uncertainty of Bayesian deep networks", Scientific Reports, Vol. 11, No. 1, 2021.

[12] B. Pandey, D. Kumar Pandey, B. Pratap Mishra, W. Rhmann, "A comprehensive survey of deep learning in the field of medical imaging and medical natural language processing: Challenges and research directions", Journal of King Saud University - Computer and Information Sciences, Vol. 34, No. 8, 2022, pp. 5083-5099.

[13] S. Atasever, N. Azgınoglu, D. S. Terzı, R. Terzı, "A comprehensive survey of deep learning research on medical image analysis with focus on transfer learning", Clinical Imaging, 2022.

[14] Z. Qiu, Y. Hu, J. Zhang, X. Chen, J. Liu, "FGAM: A pluggable light-weight attention module for medical image segmentation", Computers in Biology and Medicine, Vol. 146, 2022, p. 105628.

[15] L. Zhang, B. Zhu, C. Ma, "Utsn-Net: Medical Image Semantic Segmentation Model Based on Skip Non-Local Attention Module", SSRN Electronic Journal, 2022.

[16] P. Tang, P. Yang, D. Nie, X. Wu, J. Zhou, Y. Wang, "Unified medical image segmentation by learning from uncertainty in an end-to-end manner", Knowledge-Based Systems, Vol. 241, 2022, p. 108215.

[17] R. Wang, S. Chen, C. Ji, J. Fan, Y. Li, "Boundary-aware context neural network for medical image segmentation", Medical Image Analysis, Vol. 78, 2022, p. 102395.

[18] J. Wan, S. Yue, J. Ma, X. Ma, "A coarse-to-fine full attention guided capsule network for medical image segmentation", Biomedical Signal Processing and Control, Vol. 76, 2022, p. 103682.

[19] Z. Wu, J. Wei, J. Wang, R. Li, "Slice imputation: Multiple intermediate slices interpolation for anisotropic 3D medical image segmentation", Computers in Biology and Medicine, Vol. 147, 2022, p. 105667.

[20] X. Xie, X. Pan, W. Zhang, J. An, "A context hierarchical integrated network for medical image segmentation", Computers and Electrical Engineering, Vol. 101, 2022, p. 108029.

[21] X. Guo, C. Yang, Y. Yuan, "Dynamic-weighting hierarchical segmentation network for medical images", Medical Image Analysis, Vol. 73, 2021, p. 102196.

[22] S. Rani, "A novel mathematical morphology-based edge detection method for medical images", CSI Transactions on ICT, Vol. 4, No. 2-4, 2016, pp. 217-225.

[23] M. Lalonde, M. Beaulieu, L. Gagnon, "Fast and robust optic disc detection using pyramidal decomposition and Hausdorff-based template matching", IEEE Transactions on Medical Imaging, Vol. 20, No. 11, 2001, pp. 1193-1200.

[24] W. Chen, R. Smith, S.-Y. Ji, K. R. Ward, K. Najarian, "Automated ventricular systems segmentation in brain CT images by combining low-level segmentation and high-level template matching", BMC Medical Informatics and Decision Making, Vol. 9, No. S1, 2009.

[25] A. Tsai et al. "A shape-based approach to the segmentation of medical imagery using level sets", IEEE Transactions on Medical Imaging, Vol. 22, No. 2, 2003, pp. 137-154.

[26] J. Song, Z. Zhang, "Magnetic Resonance Imaging Segmentation via Weighted Level Set Model Based on Local Kernel Metric and Spatial Constraint", Entropy, Vol. 23, No. 9, 2021, p. 1196.

[27] A. Krizhevsky, I. Sutskever, G. E. Hinton, "ImageNet classification with deep convolutional neural networks", Communications of the ACM, Vol. 60, No. 6, 2017, pp. 84-90.

[28] M. Florkowski, "Classification of Partial Discharge Images Using Deep Convolutional Neural Networks", Energies, Vol. 13, No. 20, 2020, p. 5496.

[29] S. Budd, E. C. Robinson, B. Kainz, "A survey on active learning and human-in-the-loop deep learning for medical image analysis", Medical Image Analysis, Vol. 71, 2021, p. 102062.

[30] S. Budd, E. C. Robinson, B. Kainz, "A survey on active learning and human-in-the-loop deep learning for medical image analysis", Medical Image Analysis, Vol. 71, 2021, p. 102062.

[31] S. Asgari Taghanaki, K. Abhishek, J. P. Cohen, J. Cohen-Adad, G. Hamarneh, "Deep semantic seg-

mentation of natural and medical images: a review", Artificial Intelligence Review, Vol. 54, No. 1, 2020, pp. 137-178.

[32] H. Seo et al. "Machine learning techniques for biomedical image segmentation: An overview of technical aspects and introduction to state-of-art applications", Medical Physics, Vol. 47, No. 5, 2020.

[33] N. Tajbakhsh, L. Jeyaseelan, Q. Li, J. N. Chiang, Z. Wu, X. Ding, "Embracing imperfect datasets: A review of deep learning solutions for medical image segmentation", Medical Image Analysis, Vol. 63, 2020, p. 101693.

[34] M. H. Hesamian, W. Jia, X. He, P. Kennedy, "Deep Learning Techniques for Medical Image Segmentation: Achievements and Challenges", Journal of Digital Imaging, Vol. 32, No. 4, 2019, pp. 582-596.

[35] P. Meyer, V. Noblet, C. Mazzara, A. Lallement, "Survey on deep learning for radiotherapy", Computers in Biology and Medicine, Vol. 98, 2018, pp. 126-146.

[36] Z. Akkus, A. Galimzianova, A. Hoogi, D. L. Rubin, B. J. Erickson, "Deep Learning for Brain MRI Segmentation: State of the Art and Future Directions", Journal of Digital Imaging, Vol. 30, No. 4, 2017, pp. 449-459.

[37] T. Eelbode et al. "Optimization for Medical Image Segmentation: Theory and Practice When Evaluating with Dice Score or Jaccard Index", IEEE Transactions on Medical Imaging, Vol. 39, No. 11, 2020, pp. 3679-3690.

[38] "Data Science Bowl 2017 | Kaggle", Data Science Bowl 2017 | Kaggle. https://www.kaggle.com/c/data-science-bowl-2017. (accessed: 2022)